



UNIVERSITÀ  
DEGLI STUDI  
FIRENZE

# FLORE

## Repository istituzionale dell'Università degli Studi di Firenze

### **Theoretical and numerical assessment of an enhanced Humidification-Dehumidification desalination system based on**

Questa è la versione Preprint (Submitted version) della seguente pubblicazione:

*Original Citation:*

Theoretical and numerical assessment of an enhanced Humidification-Dehumidification desalination system based on Indirect Evaporative Cooling and Vapour Compression Refrigeration / Andrea Rocchetti; Luca Socci. - In: APPLIED THERMAL ENGINEERING. - ISSN 1359-4311. - ELETTRONICO. - 208:(2022), pp. 0-0. [10.1016/j.applthermaleng.2022.118194]

*Availability:*

The webpage <https://hdl.handle.net/2158/1283224> of the repository was last updated on 2022-10-10T12:42:41Z

*Published version:*

DOI: 10.1016/j.applthermaleng.2022.118194

*Terms of use:*

Open Access

La pubblicazione è resa disponibile sotto le norme e i termini della licenza di deposito, secondo quanto stabilito dalla Policy per l'accesso aperto dell'Università degli Studi di Firenze (<https://www.sba.unifi.it/upload/policy-oa-2016-1.pdf>)

*Publisher copyright claim:*

Conformità alle politiche dell'editore / Compliance to publisher's policies

Questa versione della pubblicazione è conforme a quanto richiesto dalle politiche dell'editore in materia di copyright.

This version of the publication conforms to the publisher's copyright policies.

La data sopra indicata si riferisce all'ultimo aggiornamento della scheda del Repository FloRe - The above-mentioned date refers to the last update of the record in the Institutional Repository FloRe

(Article begins on next page)

# Theoretical and numerical assessment of an enhanced Humidification-Dehumidification desalination system based on Indirect Evaporative Cooling and Vapour Compression Refrigeration

Andrea Rocchetti, Luca Socci

ThermoGroup, Department of Industrial Engineering, University of Florence, Italy

---

## Highlights

- A novel humidification-dehumidification desalination system is proposed.
  - An Indirect Evaporative Cooler is used both as a humidifier and cooling source.
  - A Vapour Compression Refrigeration cycle is used to enhance scheme performances.
  - The numerical study of the scheme shows competitive results in the HDH sector.
- 

## Keywords

Desalination  
Humidification-Dehumidification  
Indirect Evaporative Cooling  
Maisotsenko Cycle  
Vapour Compression Refrigeration  
Performance evaluation

## Abstract

In this work, a theoretical study and a numerical performance analysis of a novel Humidification-Dehumidification (HDH) desalination system, that simultaneously exploits an Indirect Evaporative Cooling (Maisotsenko cycle, IEC) device and a Vapour Compression Refrigeration cycle (VCR), are proposed. The IEC device is here employed as a very efficient saltwater evaporator-air humidifier, by an optimized mass exchange process between saltwater and working airstream. Both thermal exchanges of the VCR cycle are used: the hot coil pre-heats the inlet air to enhance the effectiveness of the evaporation process, while the cold one provides the cooling capacity to condense freshwater. The numerical model is based on data of actual commercial devices and considers their effective operational mode. The parametric analysis and the yearly simulations in different climatic areas show very promising results (GOR and RWA factor equal to 3.4 and  $5.0 \cdot 10^6$  in the best operative condition, equal to 3.2 and  $4.1 \cdot 10^6$  in the best climate situation) that lead to consider this technology as very competitive among HDH desalinations systems.

---

## Introduction

As it is widely known, about 97 % of water present on Earth is in the form of saltwater contained in oceans and seas, making it not suitable for human consumption [1]. Nowadays 20 % of the world population has to struggle against water scarcity, and another 25 % has not the technologies to make the available water potable [2]. Many countries worldwide are experiencing the situation of "water stress", the condition for which the whole demand for safe and usable water exceeds the supply [3]. Obtaining drinking water from "non-conventional resources" (seawater, brackish water, wastewater) is a vital necessity. In this sense, desalination of sea and brackish water is a very promising and consolidated option. Nowadays desalination plants operate in more than 120 countries all over the world, with some Mediterranean and Arabic countries that derive about 70 % of the water supply from seawater desalination [4]. As of February 2020, slightly less than 17 000 desalination plants were present, for a total installed capacity of 97.2 million m<sup>3</sup>/d and a cumulated capacity (also considering projects to be implemented) of 114.9 million m<sup>3</sup>/d [5]. Considering a global freshwater withdrawal of about  $10^{10}$  m<sup>3</sup>/d, desalination covers about the 1 % of global water need [6,7]. Recurring desalination technologies can be divided into two main categories: membrane (*reverse osmosis* and *electrodialysis*) and thermal (*multi-stage* and *multi-flash*) processes. Reverse osmosis is nowadays the leading technology, accounting for about 85 % of existing plants and about 70 % of installed capability [5,8].

## Nomenclature

### Abbreviations

c	Specific heat at constant pressure [kJ/kg/K]
COMP	Compressor of the VCR cycle
COND	Condenser of the VCR cycle
E	Energy [kWh]
e	Corrective factor of rated efficiency of VCR
EER	Energy Efficiency Ratio of VCRD
EICED	Enhanced Indirect Cooling Evaporative Desalination
EVAP	Evaporator of the VCR cycle
F, G	Numerical function of the IEC device
GOR	Gained Output Ratio
HDH	Humidification Dehumidification Desalination
HE	Air to air Heat Exchanger
IEC	Indirect Evaporative Cooling
j	Specific enthalpy [kJ/kg/K]
LAM	Lamination valve of the VCR cycle
m	Mass flow rate of air [kg/s]
M	Mass [kg]
max	Maximum
min	Minimum
P	Electric power [kW]
Q	Thermal power exchanged [kW]
q	Corrective factor of rated cooling power of VCR
r	Latent heat of vaporization [kJ/kg]
RR	Recovery ratio
RWA	Recovered Water to Air factor
S	Correlations for air at saturation

### SEC

### T

### V

### VCR

### Vol

### WE

### WR

### x

### Subscripts

### 1,2,...7

### a

### c

### d

### e

### eff

### I

### id

### II

### m

### max

### rw

### s

### w

### wb

### Greek

### ε

### ρ

Specific Energy Consumption [kWh/m<sup>3</sup>]

Dry bulbe temperature [°C]

Volumetric flow rate of air [m<sup>3</sup>/h]

Vapor Compression Refrigeration

Volume [m<sup>3</sup>]

Water evaporated [L/h]

Water recovered [kg/s]

Humidity ratio [kg/kg]

State point of the air in the scheme

Air

Condenser of VCR

Design or rated condition

Evaporator of VCR

Effective

Primary

Ideal

Secondary

Mean

Maximum

Recovered water

Saturation condition

Water

Wet Bulb

Efficiency

Density [kg/m<sup>3</sup>]

Due to the urgency of developing a solution for the water scarcity problem, scientific research and commercial companies are investigating emerging desalination technologies. Among the many, *Humidification Dehumidification* (HDH) desalination is receiving increasing interest thanks to its ability to replicate the natural water cycle - seawater evaporation that condenses freshwater into cloud and rain - using humid air as the carrier for heat and mass transfer. HDH is indeed based on saltwater vaporization into a carrier gas (generally ambient air) and then condensing part of the vapour content of the carrier gas by using a colder source. The condensed water is almost pure.

In its easiest form, an HDH scheme requires the presence of a humidifier and a dehumidifier [9]. In the humidifier, an air stream is put in contact with a saltwater flow, then mass and energy exchanges occur. In particular, water evaporates increasing the humidity ratio of air. Since the vapour tension of salts dissolved in water is much lower than water's one, only the pure water evaporates in the air. This is then cooled in the dehumidifier by a fluid at lower temperature (often a saltwater stream). During the cooling,

dehumidification happens (as long as the temperature of the coolant is lower than air stream dew point temperature), so it is possible to recover part of the water previously evaporated, obtaining the freshwater. Considering the two processes of evaporation and condensation, HDH systems can be then included in the family of thermal desalination technologies. These systems are generally very simple and involve devices that do not need extensive maintenance as membrane-based processes. They do not have limitations dictated by water quality (high salinity), can employ low-grade energy (industrial energy waste, solar energy, etc.) to improve humidification process and are generally sized for small-scale applications due to the high specific volume of air and the low values of maximum water content in the air [10].

In order to discuss and compare solutions and results of some previous works that have been found in the literature, some efficiency indices necessary to characterize an HDH plant are here introduced:

- *Gained Output Ratio* (GOR), the ratio of the latent heat of evaporation of the distilled water to the total energy input. This is a dimensionless parameter that accounts for system efficiency and the energy input is generally considered as the total amount of primary energy provided.
- *Specific Energy Consumption* (SEC), expressed in kWh of input energy consumed divided by the m<sup>3</sup> of distilled water, is the ratio of the total energy input to the total production of distilled water. It can be regarded as the dimensional inverse of GOR.
- *Recovery Ratio* (RR), a dimensionless parameter based on the ratio of the distilled water to the water circulating in the plant, or the *Recovered Water to Air factor* (RWA), based on the ratio of distilled water to the circulating air in the plant. Both parameters influence the sizing of the plant and are referred to a desalination system based on water or air as the carrier of energy or mass.

Another important dimensionless parameter is the *Mass flow Ratio* (MR), which does not describe the performances of an HDH scheme but characterizes its functioning: it is defined as the ratio between the quantity of saltwater entering the plant and the quantity of air put in contact with it.

Values of GOR, evaluated with the thermal energy input, reported in the literature, are quite low for simple HDH schemes. For example, Zubair et al. [11] reported a maximum value of GOR approximately equal to 0.5 for the open air-open water, with the water that is heated to enhance the mass and energy transfer at the humidification device. Better results, in the same work, have been obtained with the recirculation of brine in the main saltwater stream.

Starting from the easiest form of HDH, many improvements could be applied: the loop of air or/and water may be closed or a heat exchanger may be used to heat air or water [12,13]. A schematization is reported in Table 1.

**Table 1. Summary of common HDH plants configuration.**

<b>Typology of HDH</b>	<b>Air path</b>	<b>Water path</b>	<b>Air at humidifier inlet</b>	<b>Water at humidifier inlet</b>
CAOW WH	Closed	Open	Not heated	Heated
CAOW AH	Closed	Open	Heated	Not heated
CWOA WH	Open	Closed	Not heated	Heated
CWOA AH	Open	Closed	Heated	Not heated

According to Sharqawy et al. [12], for the water-heated cycle, the best performances are obtained when the quantity of salt water is much higher than the quantity of air (mass flow ratio greater than 1), while for the air-heated cycle it is better to maintain a mass flow ratio lower than 1. The Author reported a maximum

GOR of 1.9 and 2.5 for CAOW WH and CAOW AH under the best operative conditions. Narayan et al. [10] obtained similar values, that could be higher under particular conditions (in the CAOW WH for high inlet seawater temperature). According to another work of Narayan et al. [13], the CAOW WH with multiple humidification stages configuration leads to the best results among the different schemes.

Many authors have also proposed to split the humidification process into several stages to enhance the evaporation of water in the air stream [14, 15].

With the aim to improve the humidification process and the possibility to recover more pure water from the humidified air, a novel HDH desalination configuration is proposed by the Authors as the central theme of this paper. This configuration is based on the simultaneous utilization of two technologies derived from air conditioning and refrigeration applications: the Indirect Evaporative Cooling (IEC) and the Vapour Compression Refrigeration Cycle (VCR).

An IEC is substantially a heat and mass exchanger, where an airstream (*working* or *secondary air*), that is humidified by external water, can cool another air stream (*product* or *primary air*) through an exchange surface. In the past, this simple scheme has been involved in several optimization steps, generally to increase its ability to provide cooled dry air. The most important innovation is related to the *Maisotsenko-cycle* (M-Cycle). In a M-Cycle device, inlet air is cooled below its wet bulb temperature, moving towards the dew point, and part of it, exiting the device, is used as the source of secondary air [16]. A typical M-Cycle configuration is based on a heat and mass exchanger with alternate dry and wet channels. In Figure 1 a representation of the M-Cycle exchanger and processes is presented.

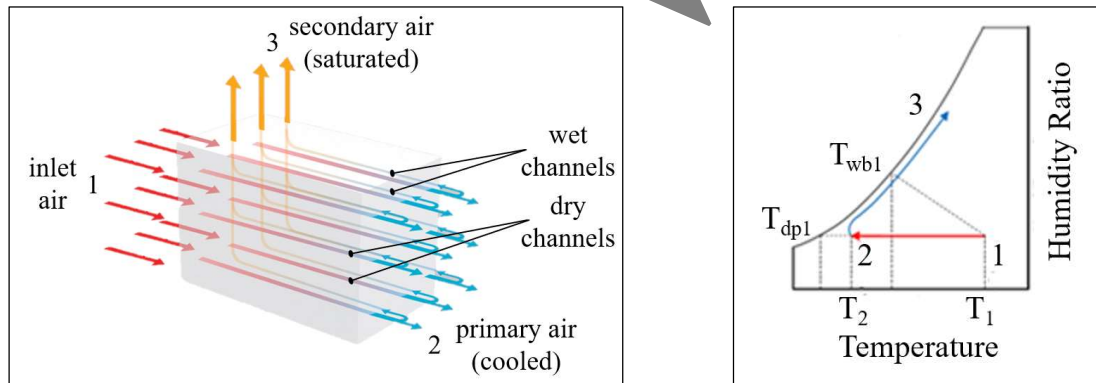


**Figure 1. Scheme of M-Cycle IEC device (left) and processes of air on psychrometric chart (right) [Courtesy of Seeley International].**

The secondary air flows through the wet channels, where the air is humidified by the evaporation of the water that wets the channels. Through the heat exchange surface, it can cool the air that flows in the dry channels. The air cooled at constant humidity ratio in the dry channels is divided, at the exit of the device, in two flows: the *primary air*, for the cooling utilization, and the *secondary air*, reversed into the wet channels where is humidified at saturation. Reversing the cooled air in the wet channels, as source of the secondary one, drastically improves the cooling performance of the device. Thinking to the original application of IEC technology, the ability to produce fresh air is the most commonly used effect, whereas the humidified stream is rejected. Conversely, this latter stream can usefully be employed in an HDH desalination scheme, efficiently accomplishing the humidification process.

In literature some examples of utilization of Indirect Evaporative Cooling, in particular the M-Cycle, in the field of water desalination/distillation have been found. Mahmood et al. [16] and Pandelidis et al. [17] underlined that a possible application of the M-cycle is the desalination of water through humidification in

wet channels and the following condensation employing the cooling power obtained thanks to the dry channels. Kabeel et al. [18] tested in a small scale application a prototype in which the secondary air of an IEC is the saltwater carrier: it is pre-humidified in the wet channels of IEC and it goes through dedicated humidification after heating within a solar collector, while the primary air is employed as cooling medium for a building. A very interesting RWA factor of about 0.01 L/h of distilled water to m<sup>3</sup>/h of secondary air, under the best-operating conditions of the plant, has been obtained. Chen et al. [19] proposed a pre-humidification and heating of carrier air in the wet channels of an IEC based on M-Cycle, then the secondary air continues its path in a water heated HDH cycle. The maximum RWA reported is about 0.15 L/h of distilled water per m<sup>3</sup>/h of secondary air, the GOR is about 2.5 in the best operative condition. Tariq et al. [20] proposed the utilization of an M-Cycle exchanger as an air saturator. It is important to underline that this publication considers in the GOR calculation the energy for air movement, which is generally neglected and, on the contrary, is the principal energy need of this system. He also made an analysis of the proposed system in different sites of the world, obtaining a maximum GOR just under 1. From this work, a key fact emerges: the higher the inlet air temperature at the IEC is, the higher the water recovery. Pandelidis et al. [21] showed a very innovative and original solution, with two or three stages of IEC used both as humidifier and dehumidifier. He also conducted a climate analysis of the desalination scheme obtaining very good results as SEC and RWA parameters, even if, according to who is writing, the presented performance indices values seems to be too optimistic, being better than a compared reverse osmosis configuration.

Moreover, the utilization of a Vapour Compression Refrigeration (VCR) cycle in an HDH scheme has been studied by many Authors. Generally speaking, VCR is placed in an HDH system with two different modes and scopes. Some Authors employ VCR to produce in the same time pure water and cooled air, other propose VCR only to enhance HDH configurations performances. In its review, Faegh underlines that VCR could be coupled with HDH, with the target to produce simultaneously desalinated water and cooling power [9]. Nada et al. have published many works on the topic [22, 23, 24, 25]. In these works, the outside air is humidified with saltwater, then flows through the evaporator of a VCR where it is cooled (to be sent to a building for air conditioning) and part of the evaporated water is recovered through condensation. From [22] emerges that the higher the inlet air humidity ratio at the evaporator of VCR is, the higher the distilled water production. The same conclusions are obtained in the other works of this Author: the increase in outdoor air temperature and humidity leads to enhance distilled water production and energy consumption. Lawal et al. studied the integration of VCR inside both water-heated and air-heated HDH cycles [26, 27]: the condenser is the heat source for water or air, while the evaporator cools the saltwater that will be used as the coolant at the dehumidifier. The air heated cycle has shown better performances, even if the water heated one is preferable as it is easier to achieve the heat exchanges involved in the process.

In this paper, a novel HDH scheme that combines the benefits of both IEC and VCR is proposed. The indirect evaporative cooler, generally used in air conditioning applications, is here exploited as a very efficient saltwater evaporator-air humidifier, by the optimized mass exchange process between saltwater and working airstream. The secondary air can be humidified by using seawater, while the primary air can be used as a cooling medium in an air-to-air heat exchanger to dehumidify the other stream, recovering freshwater. If a VCR cycle is coupled to the system composed by the IEC and the heat exchanger, the desalination performances can be improved: the hot coil pre-heats the inlet air enhancing the effectiveness of the evaporation process, while the cold coil provides the additional cooling capacity to recover

freshwater. The configuration has been named by the Authors *Enhanced Indirect Cooling Evaporative Desalination* (EICED) system. The scheme is theoretically presented, numerically simulated and subjected to a parametric analysis; also a performance hourly analysis in different sites of the world, according to Koppen climate classification, has been done. The IEC has been analysed with the data provided by an established Manufacturer that collaborates with the Authors' Research Group. The VCR has been studied using models from the technical literature, derived from real devices according to test standards of important associations as ASHRAE and AHRI. To the best of the Authors' knowledge this configuration, with the simultaneous utilization of IEC and VCR in an HDH desalinator, is not present in the literature and has never been simulated before. The results obtained are very encouraging, suggesting that such a scheme can well perform in almost any global climate context.

### Scheme of the proposed EICED configuration

In Figure 2 a representation of the proposed EICED scheme is shown; the components of a traditional VCR cycle are also shown. In Figure 3 the processes that air streams undergo in the EICED scheme are represented in an indicative psychrometric chart.

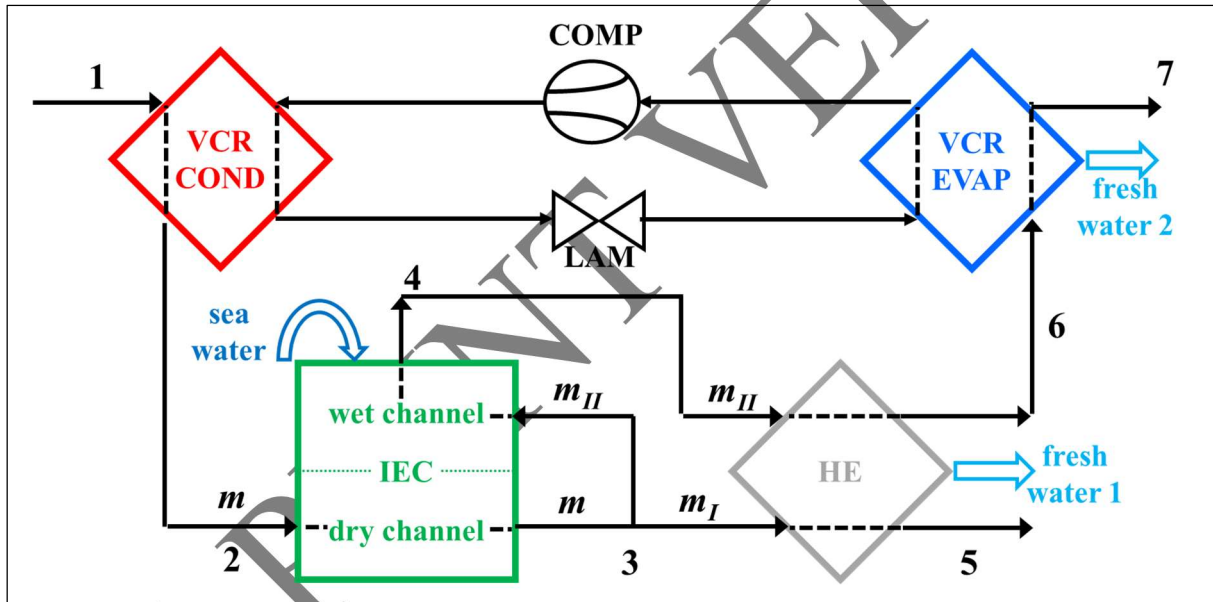
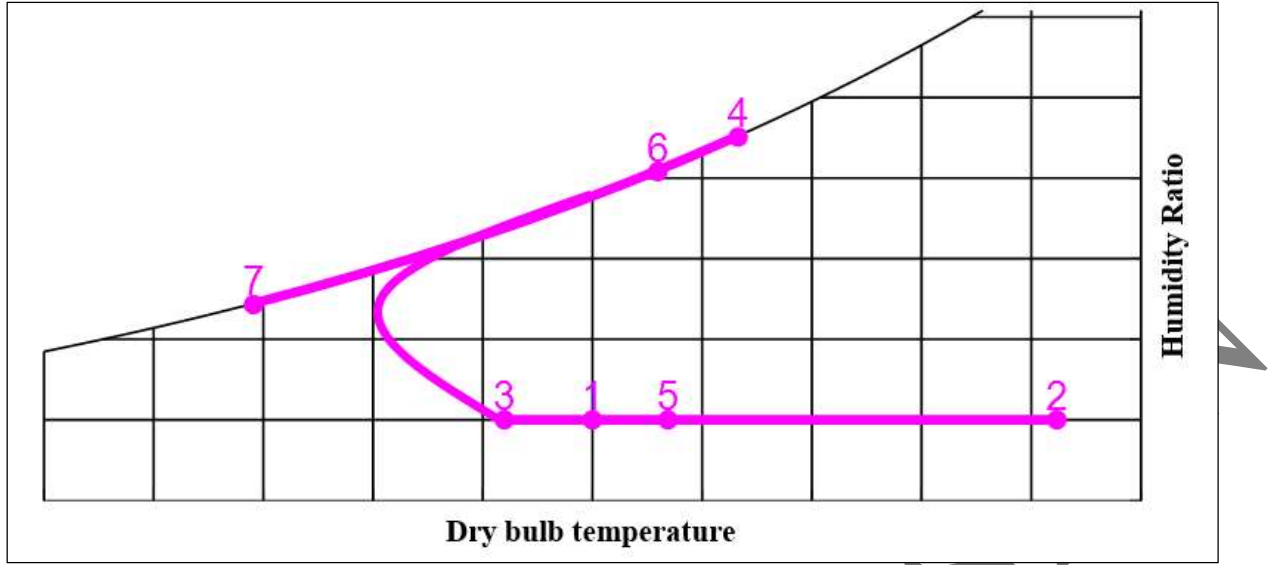


Figure 2. Representation of the proposed EICED system.



**Figure 3. Representation of the psychrometric processes of air in the proposed EICED system.**

The outdoor air (point 1), before entering the IEC, is heated by the condenser of the VCR (1-2). It enters the dry channels of IEC and is sensibly cooled (2-3). Part of the air is reversed through the wet channels, where it is simultaneously humidified by the evaporation of saltwater and heated by the heat transfer from the primary air (3-4). If the primary air is colder than the secondary one (that happens in most situations simulated), the heat exchanger (HE) is activated, with heating of the primary air (3-5) and pre-cooling and pre-dehumidification of the secondary air (4-6): here part of the water is recovered and then the secondary air is cooled and dehumidified at the evaporator of the VCR (6-7) with additional recovery of distilled water.

### Mathematical model

In this section, the mathematical model of the overall EICED system is presented. Subscripts in the equations are referred to the schemes in Figure 2 and Figure 3.

Outdoor air entering the plant is sensibly heated at the condenser:

$$Q_{c,VCR} = c_a \cdot m \cdot (T_2 - T_1) \quad (1)$$

$$x_2 = x_1 \quad (2)$$

where  $m$  is the sum of primary and secondary air flow rate of the IEC:

$$m = m_I + m_{II} \quad (3)$$

$$m = \frac{\rho_a \cdot V}{3\,600} \quad (4)$$

where 3 600 is expressed in [s/h].

The IEC device operates the following psychrometric transformations on the primary and the secondary air:

$$T_3 = F_{IEC} (T_2, x_2) \quad (5)$$

$$x_3 = x_2 \quad (6)$$

$$T_4 = G_{IEC} (T_2, x_2) \quad (7)$$

$$x_4 = S_{TX} (T_4) \quad (8)$$



where  $F_{IEC}$  and  $G_{IEC}$  are numerical functions that calculate the outlet condition of the primary and secondary streams, according to the mass and energy balances of the IEC system. These functions are built on operational data certified by the Manufacturer [28, 29].  $S_{Tx}$  is a function (based on Antoine's Law) that relates the temperature at saturation conditions to the humidity ratio. The quantity of water evaporated in the wet channels of IEC is expressed as:

$$WE_{IEC} = m_{II} \cdot (x_4 - x_3) \quad (9)$$

Since the primary air has a temperature lower than the secondary one, it is able to pre-cool and pre-dehumidify of the secondary air at the air-to-air heat exchanger. The heat exchanged between the two air streams is determined considering the Kays efficiency of the heat exchanger and evaluating the maximum exchangeable heat:

$$Q_{eff} = \varepsilon_{HE} \cdot Q_{max} \quad (10)$$

$$Q_{max} = \min(Q_{maxI}, Q_{maxII}) \quad (11)$$

$$Q_{maxI} = m_I \cdot (j_{5,id} - j_3) \quad (12)$$

$$Q_{maxII} = m_{II} \cdot (j_4 - j_{6,id}) \quad (13)$$

where  $j_{5,id}$  is evaluated at  $T=T_4$  and  $x=x_3$ , while  $j_{6,id}$  is evaluated at  $T=T_3$  and saturation. The outlet conditions of secondary air are:

$$j_6 = j_4 - Q_{eff}/m_{II} \quad (14)$$

$$T_6 = S_{jT}(j_6) \quad (15)$$

$$x_6 = S_{jx}(j_6) \quad (16)$$

where  $S_{jT}$  and  $S_{jx}$  are the functions that relate the specific enthalpy at saturation to temperature and humidity ratio. The recovered water at the air-to-air heat exchanger is then:

$$WR_{HE} = m_{II} \cdot (x_4 - x_6) \quad (17)$$

The air entering the evaporator of the VCR undergoes a cooling with dehumidification. The cooling power of the VCR is evaluated as follows:

$$Q_{e,VCR} = Q_{e,d} \cdot q \quad (18)$$

where the corrective factor  $q$  can be calculated through a biquadratic expression function of the wet-bulb temperature of inlet air to the evaporator and the dry bulb temperature of condensing air.

So the psychrometric conditions of evaporator outlet air can be defined:

$$j_7 = j_6 - Q_e/m_{II} \quad (19)$$

$$T_7 = S_{jT}(j_7) \quad (20)$$

$$x_7 = S_{jx}(j_7) \quad (21)$$

The recovered water at the evaporator of the VCR is:

$$WR_{VCR} = m_{II} \cdot (x_6 - x_7) \quad (22)$$

So the total recovered water is:

$$WR = WR_{HE} + WR_{VCR} \quad (23)$$

During its functioning, the VCR absorbs an electric power equal to:

$$P_{VCR} = Q_{e,VCR} / EER \quad (24)$$

The coefficient of performance can be written as:

$$EER = \frac{EER_d}{e} \quad (25)$$

where the corrective factor  $e$ , also assessed by a biquadratic function similar to that of  $q$ , can be used to modulate the nominal  $EER$  ( $EER_d$ ) to consider the actual operating condition of the VCR. So it is possible to calculate the thermal power that the VCR device provides to the air entering the plant as:

$$Q_{c,VCR} = Q_{e,VCR} + P_{VCR} \quad (26)$$

Equations that describe the VCR cycle are based on the modelling proposed by the manual of the thermodynamic simulation code *Energy Plus* [30], relying on ASHRAE (*American Society of Heating, Refrigerating and Air-Conditioning Engineers*) and AHRI (*Air Conditioning, Heating, and Refrigeration Institute*) standards.

The equation (1) depends on (26), so an iterative method is needed to solve the system of equations. A  $T_2$  temperature is assumed, in order to evaluate the  $Q_{c,VCR}$  with equation (1), then all the equations are solved. The  $Q_{c,VCR}$  evaluated with equation (26) is compared with  $Q_{c,VCR}$  obtained by equation (1). Iteration on  $T_2$  is carried out until the absolute difference between  $Q_{c,VCR}$  values evaluated with equations (1) and (26) is lower than a fixed tolerance ( $10^{-3}$  kW).

The software *Matlab*, version *R2021a*, has been used to write and solve a numerical code that contains all the equations that simulate the scheme.

According to the definition given in the Introduction of this work, the performance indices of the plant can be expressed as:

- *Gained Output Ratio*

$$GOR = \frac{M_{rw} \cdot r_w}{3600 \cdot (E_{IEC} + E_{VCR})} \quad (27)$$

where  $M_{rw}$  is the total amount of recovered water during the simulation period (the sum of recovered water at HE and evaporator of VCR),  $E_{IEC}$  and  $E_{VCR}$  are the electric energy consumption of IEC and VCR during the simulation period

- *Specific Energy Consumption*, (it can be seen as the inverse of GOR)

$$SEC = \frac{E_{IEC} + E_{VCR}}{Vol_{rw}} \quad (28)$$

- *Recovered Water to Air factor*, the ratio of the recovered water to the volumetric airflow entering in the plant

$$RWA = \frac{WR \cdot 3600}{\rho_w \cdot V} \quad (29)$$

Temperature and humidity ratio of inlet air are variable. A reference atmospheric pressure of 101 325.0 Pa has been considered. Constant values for air specific heat at constant pressure and density have been chosen, equal to 1 kJ/(kg·K) and 1.2 kg/m<sup>3</sup>. For saltwater, values for latent heat of vaporization and density are constant, equal to 2 500 kJ/kg and 1 000 kg/m<sup>3</sup>. The salinity level of common seawater does not affect the evaporation and cooling phenomena, so it is possible to consider saltwater as pure water.

The following input parameters for IEC and VCR devices have been used:

**Table 2. Input parameters for IEC and VCR devices.**

$\dot{m}_I$ [kg/s]	1.32
$\dot{m}_{II}$ [kg/s]	1.08
$P_{IEC}$ [kW]	1.8
$Q_{e,d}$ [kW]	17.0

The biquadratic functions that express the corrective factors  $q$  and  $e$  are in the forms:

$$q \text{ (or } e) = k_0 + k_1 \cdot T_{wb6} + k_2 \cdot T_{wb6}^2 + k_3 \cdot T_1 + k_4 \cdot T_1^2 + k_5 \cdot T_{wb6} \cdot T_1 \quad (30)$$

where the coefficients of the functions are assigned as follow:

**Table 3. Coefficients of biquadratic function for  $q$  and  $e$  VCR device corrective factors.**

	$q$	$e$
$k_0$	0.9953455	0.3802131
$k_1$	-0.0118418	0.0199468
$k_2$	0.0012277	-0.0006682
$k_3$	0.0030246	0.0058933
$k_4$	-0.0000702	0.0004646
$k_5$	-0.0003685	-0.0004072

These coefficients are based on the actual performance of commercial devices [31, 32, 33].

## Results and discussion

A parametric analysis of the proposed scheme is presented as a general survey of the potential performance of the system. Influencing parameters are temperature and humidity ratio of air entering the plant. The numerical model considers each device's operational performance referred to an actual technology level; moreover, an analysis of the influence of the rating efficiencies of these devices is considered. The potential of the plant is evaluated by the performance indices (GOR, SEC, RWA). An analysis of the performance considering the location in different sites of the world is also presented.

### Parametrical analysis

An evaluation of GOR, SEC and RWA varying inlet air temperature and humidity ratio has been conducted, over a temperature range of 10.0 - 40.0 °C and a humidity ratio range of 2.0 - 20.0 g/kg. This choice has been dictated by the following reasons:

- The Manufacturer suggests 60°C as the maximum inlet temperature at the IEC. An upper limit at 40°C for the inlet air guarantees, from the results of our simulation, to remain within the limit notwithstanding the additional heating produced by the VCR condenser.
- The low temperature limit is posed to prevent low efficiency at VCR, but also to respect a range admissibility of the IEC operational maps on which  $F_{IEC}$  and  $G_{IEC}$  numerical functions are based;
- A humidity ratio greater than 20.0 g/kg is rarely observed in most climates around the world.

The effect of inlet air temperature and humidity ratio on GOR, SEC and RWA is shown in Figure 4, Figure 5 and Figure 6.

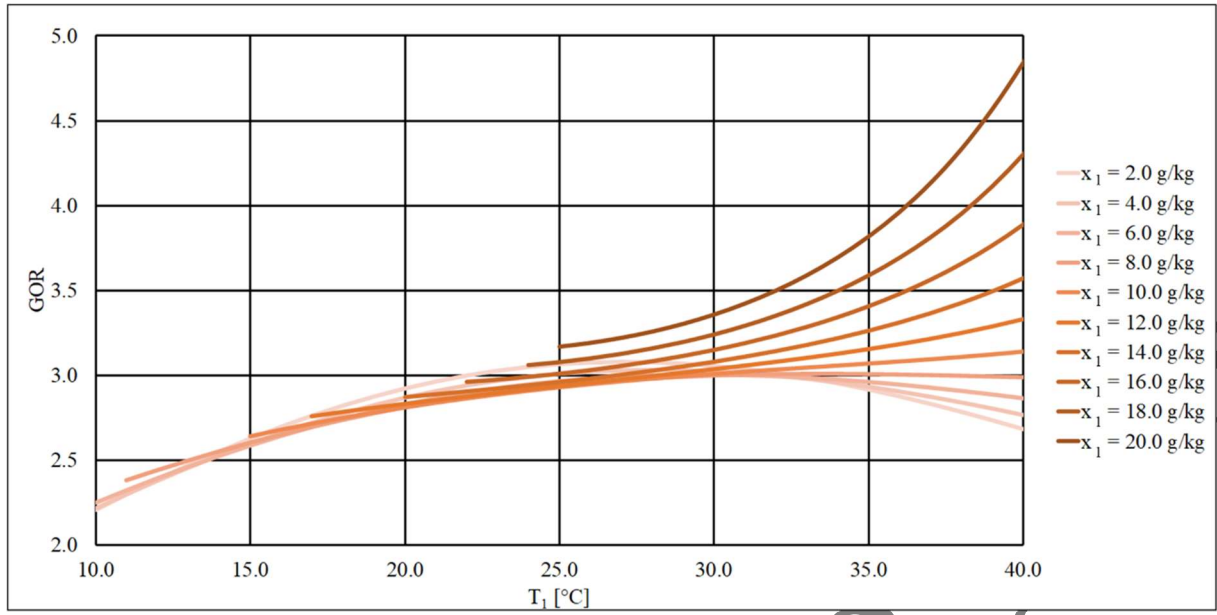


Figure 4. Effect of inlet air temperature and humidity ratio on GOR ( $\epsilon_{HE}=0.70$ ,  $EER_d=3.0$ ).

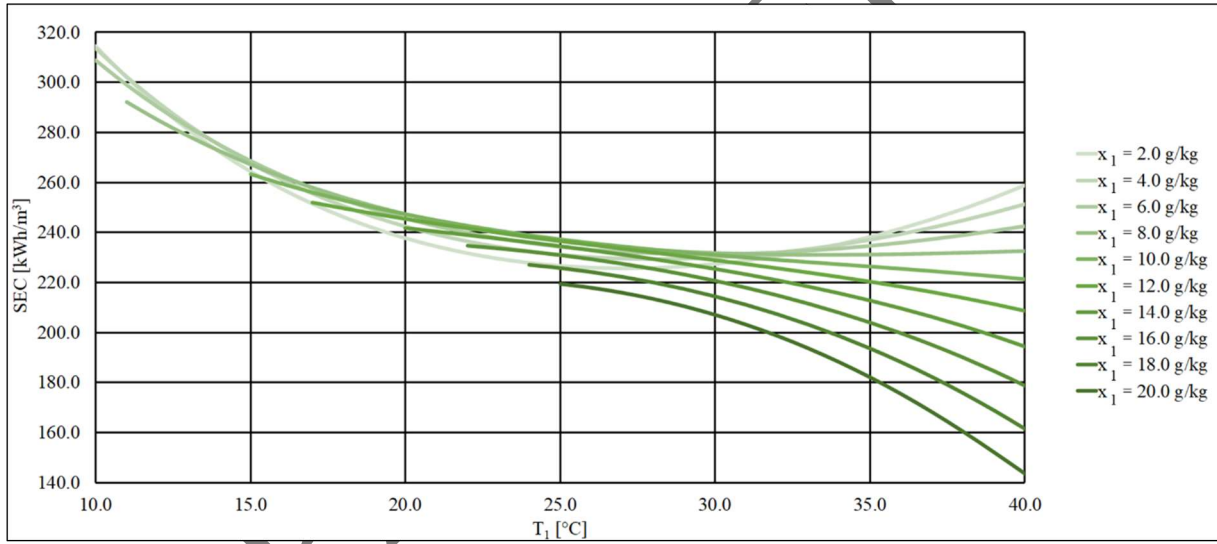
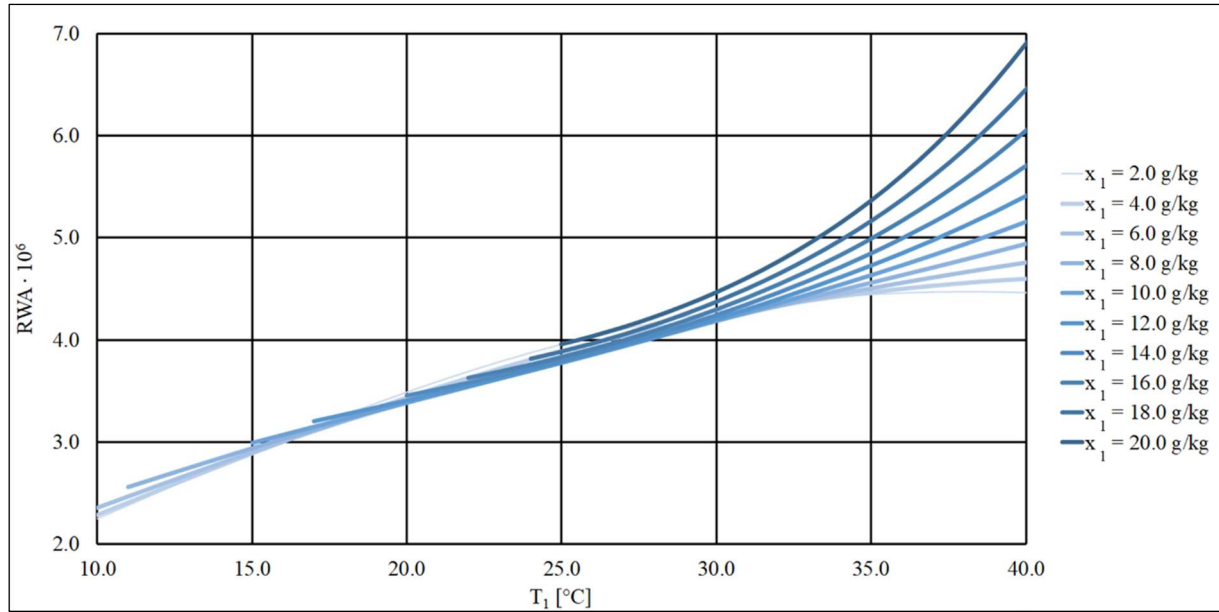


Figure 5. Effect of inlet air temperature and humidity ratio on SEC ( $\epsilon_{HE}=0.70$ ,  $EER_d=3.0$ ).



**Figure 6. Effect of inlet air temperature and humidity ratio on RWA ( $\epsilon_{HE}=0.70$ ,  $EER_d=3.0$ ).**

Improved performances of the plant (high GOR and RWA, low SEC), are obtained for high values of inlet air temperature with a high humidity ratio. For lowest values of inlet air humidity ratio (below 6.0 g/kg), curves of GOR (SEC) present a trend with a maximum (minimum); so for these levels of humidity an optimum of functioning exists (noted at  $T=27.0$  °C for  $x=2.0$  g/kg,  $T=28.5$  °C for  $x=4.0$  g/kg,  $T=30.0$  °C for  $x=6.0$  g/kg); for a humidity ratio above 8.0 g/kg, performance curves become monotonous (increasing for GOR, decreasing for SEC), so in the medium-high range of humidity the plant will improve its performance increasing the inlet air temperature. To clarify this behaviour it is then important to consider the system response at three different inlet air conditions (test points):

- Condition A: low temperature, low humidity ratio.
- Condition B: high temperature, low humidity ratio.
- Condition C: high temperature, high humidity ratio.

Figure 7 shows on the psychrometric chart the air processes that the inlet air undergoes and Table 4 presents the most important parameters, in order to evaluate the desalinations system performance.

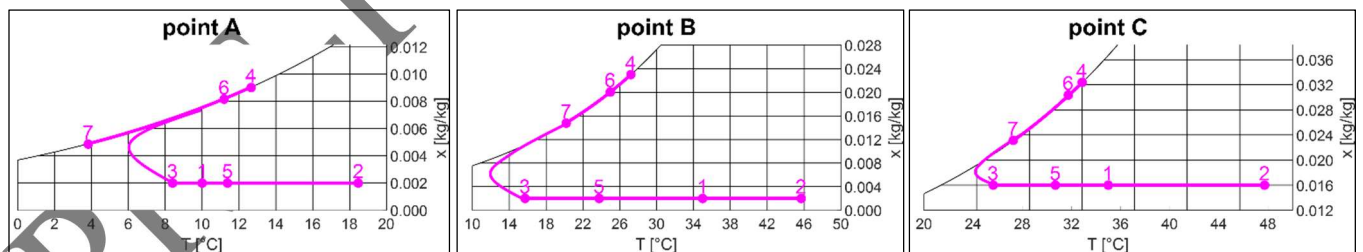


**Figure 7. Psychrometric chart representation of the processes of air at test points ( $\epsilon_{HE}=0.70$ ,  $EER_d=3.0$ ).**

**Table 4. Performance of the scheme at test points ( $\epsilon_{HE}=0.70$ ,  $EER_d=3.0$ ).**

Test Point	$T_1$ [°C]	$x_1$ [g/kg]	IEC Water evaporated [L/h]	VCR EER	GOR	$RWA \cdot 10^6$	$WR_{HE}/WR$ [%]
A	10.0	2.0	27.3	5.2	2.2	2.2	20.7
B	35.0	2.0	81.7	3.4	2.9	4.4	35.6
C	35.0	16.0	63.7	4.5	3.4	5.0	21.9

When inlet air is at the lowest temperatures (and low humidity ratios, point A) the amount of water evaporated in the air by the IEC device is small, notwithstanding the favourable effect of the heating power provided by the high-temperature source of the VCR. If the thermodynamic conditions of the airstreams at the HE inlet ports are quite close then the water recovery at the HE is also small. Despite the temperature difference at the VCR thermal sources is low ( $T_2-T_7$ ), which provides a high EER, the low value of the air temperature at the inlet of the evaporator, below its reference values, causes a low cooling power at the evaporator that precludes a high water recovery. The overall RWA is low and this effect is predominant: the GOR is also low. Inlet air stream at high temperatures and low humidity ratios (point B) are the optimal inlet air conditions to obtain better IEC performance. The thermodynamic conditions of the air streams at the HE inlet ports are more favourable than in test point A, so a greater water recovery at the HE is achievable. On the other hand, these inlet air conditions are not so good for the VCR device: high temperature difference at the VCR thermal sources results in a low EER. Nevertheless, test point B shows favourable index parameters: RWA and GOR are both greater than at test point A. Inlet air stream at high temperatures and high humidity ratios (point C) provides an optimal performance, integrating the favourable effects in test point B with an improved performance of the VCR due to the marginal temperature difference at the VCR thermal sources that produces a high EER.

Additional parametric analysis is proposed, still based on the same mathematical model and same three test points, by varying the nominal values of  $EER_d$  and  $\varepsilon_{HE}$ . Results are shown in terms of GOR and RWA for the three test points.

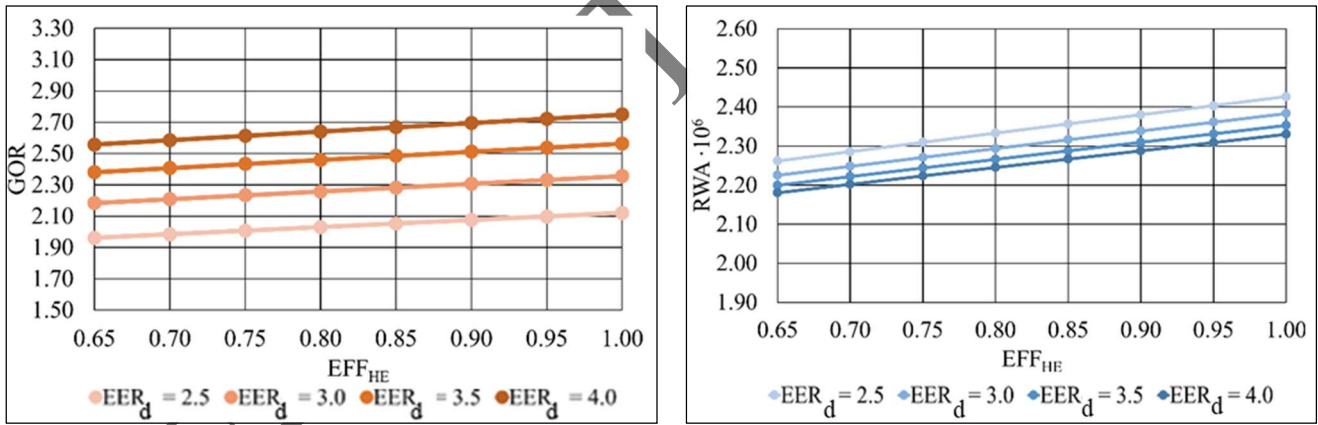


Figure 8. Effects of  $EFF_{HE}$  and  $EER_d$  on GOR and RWA for test point A.

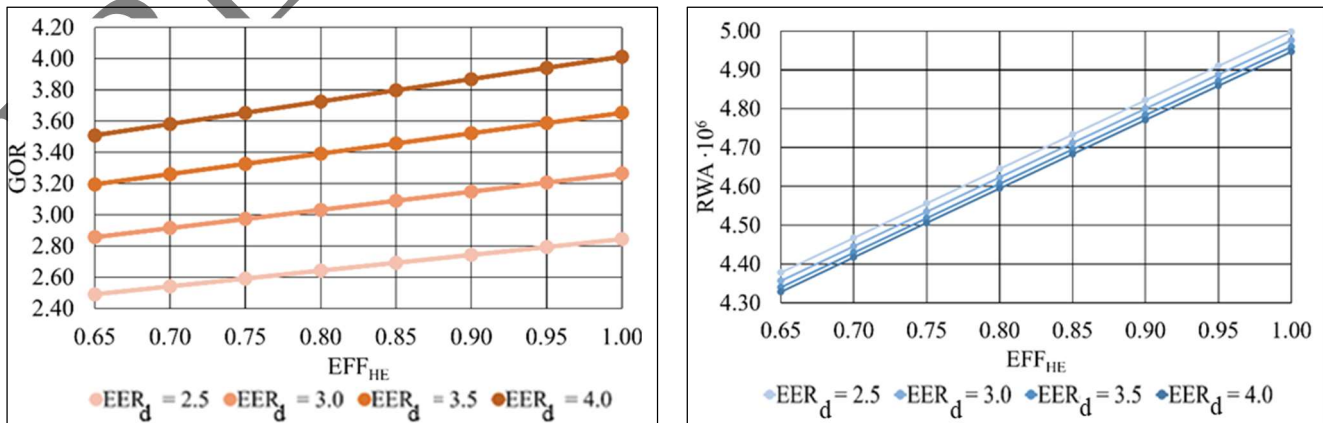
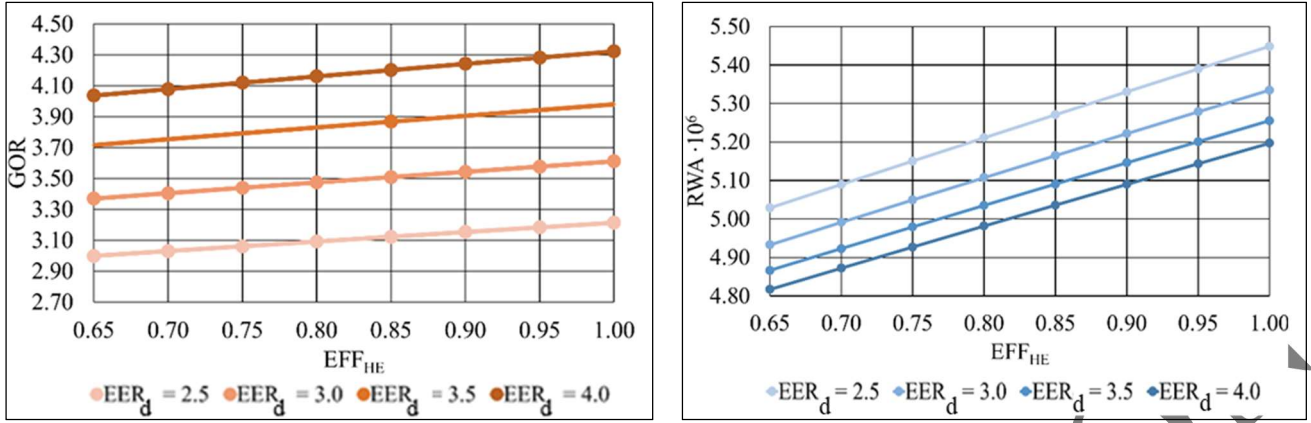


Figure 9. Effects of  $EFF_{HE}$  and  $EER_d$  on GOR and RWA for test point B.



**Figure 10. Effects of  $EFF_{HE}$  and  $EER_d$  on GOR and RWA for test point C.**

A greater nominal  $EER_d$  highly improves the GOR in test points B and C, while it has a low positive influence on test point A. Conversely, it reduces the RWA for all the test points considered. The effect of  $EER_d$  on RWA can be explained using this point of view: at higher design  $EER_d$  (so at higher EER also in the operating condition), lower thermal power is provided at the VCR condenser, resulting in a colder air entering the IEC and in a disadvantaged evaporation rate in the wet channels. This result underlines the importance to work with hot air entering the IEC: in this sense, an air pre-heating with other (eventually renewable) sources can be a critical option. Regarding the importance of  $e_{HE}$ , it strongly controls the overall performance for test point B. This point represents a very good condition for IEC device operation: an high quantity of water is evaporated in the wet channels, resulting in a very humid secondary air, and a cold primary air is produced. So it is possible to recover much freshwater with the air-to-air heat exchanger, as long as it has an high efficiency. From Table 4 is possible to note indeed that, in test point B, the water recovery occurs for 35 % in the heat exchanger, much more than in other test points.

### Feasibility in different locations

The influence of different climatic condition has been investigated, the outdoor air being the inlet mass flow rate to the system. The operational performance of the scheme has been simulated taking into account the local conditions of different coastal cities in the world, belonging to the various classes of Koppen climates classification [34]. An analysis has been done using the hourly climatic data extended to all hours of the year (database of climatic data by Energy Plus [35]). The simulations have been performed considering the activation of the plant when the outdoor specific enthalpy is greater than 10.0 kJ/kg. The simulation results of ten different cities in ten Koppen's regions are shown in Table 5, when the efficiency of the heat exchanger is 0.7 and the nominal  $EER_d$  of the VCR is 3.0.



**Table 5. Performance analysis of the propose EICED system for different sites according to Koppen classification.**

Region/Site	$T_m$	$x_m$	GOR	SEC	$RWA \cdot 10^6$	$WR_{HE}/WR$ [%]
<b>Group A: Tropical climates</b>						
<i>A1: Tropical rainforest</i>						
Singapore (Singapore)	27.5	0.0180	3.15	220.20	4.10	13.40
<i>A2: Tropical monsoon</i>						
Rio de Janeiro (Brasil)	24.0	0.0129	2.94	236.08	3.70	18.31
<i>A3: Tropical savanna</i>						
Miami (USA)	24.5	0.0120	2.96	234.41	3.80	20.71
<b>Group B: Dry climates</b>						
<i>B1: Hot semi-arid</i>						
Tripoli (Libya)	20.3	0.0068	2.76	251.57	3.40	27.53
<i>B2: Cold semi-arid</i>						
Valencia (Spain)	17.3	0.0063	2.69	258.00	3.10	28.86
<i>B3: Hot desert</i>						
Abu Dhabi (UAE)	27.1	0.0096	2.98	232.67	4.00	22.87
<b>Group C: Temperate climates</b>						
<i>C1: Humid subtropical</i>						
Brisbane (Australia)	20.0	0.0083	2.81	247.24	3.40	19.87
<i>C2: Temperate oceanic</i>						
Auckland (New Zealand)	15.3	0.0069	2.59	268.42	2.90	22.14
<i>C3: Warm Mediterranean</i>						
Barcelona (Spain)	15.7	0.0068	2.61	266.42	3.00	22.18
<i>C4: Temperate Mediterranean</i>						
Cape Town (South Africa)	16.5	0.0065	2.66	261.47	3.10	25.15

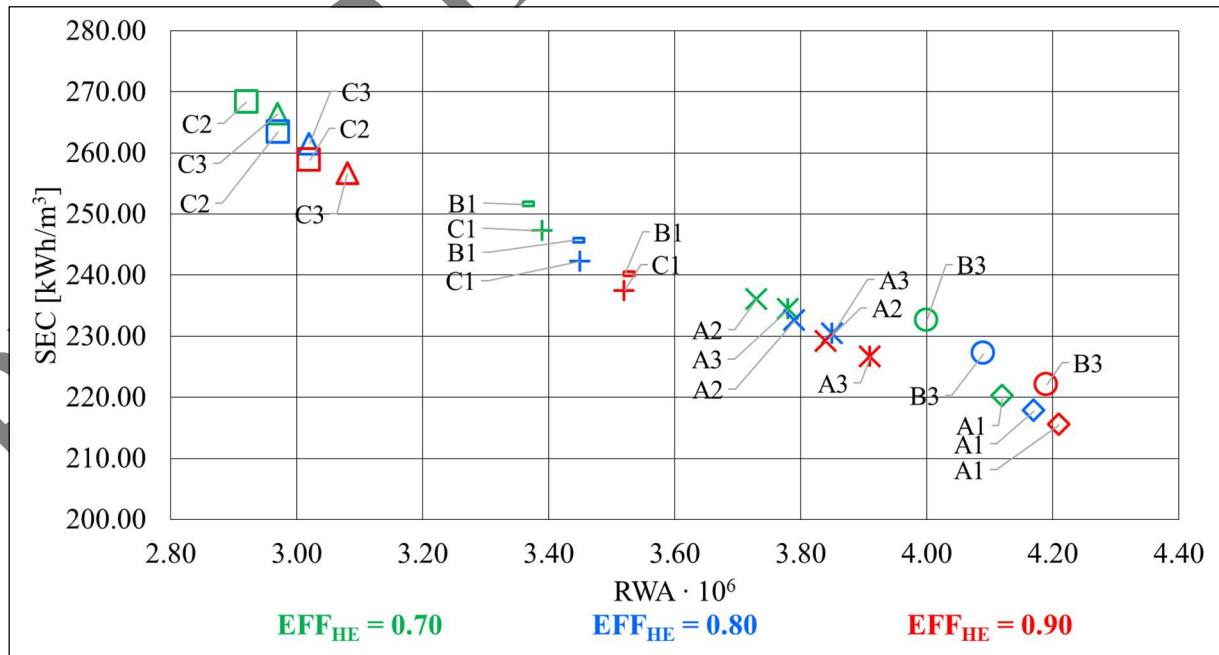


**Figure 11. Performances of the proposed EICED system in different climate regions of the world.**



From the Table 5 and the Figure 11, it is possible to note that the performances of the plant are considerably high. All of these climates are characterized by middle-high temperatures, confirming the importance to have high air temperature entering the plant, as evident from the parametrical analysis. The same parametrical analysis shows that the best performance is obtained in a hot humid climate as Singapore one, where it is possible to obtain a GOR of 3.15. As it has been done in the parametrical analysis, the repartition of water recovered between the heat exchanger and the evaporator has been evaluated. With the yearly simulations, what has been observed by the parametric analysis is confirmed:

- In humid climates (i.e. Singapore or Rio de Janeiro), the water recovery at the air-to-air heat exchanger is not relevant and it is mainly carried out by the cold coil of VCR cycle; indeed, the primary and the secondary air streams of IEC have close temperatures, resulting in a limited heat transfer and dehumidification at the HE.
- In dry climates (i.e. Tripoli or Abu Dhabi), where the primary air has a temperature much lower than the secondary one, the heat subtracted to the secondary air is high and then the water recovery at the heat exchanger increases.

It is crucial to underline that only the utilization of VCR device leads to obtain high performances in all climates, as the next Figure 12 demonstrates. It shows the performances, in terms of RWA and SEC for the same sites of the world, when the VCR cycle is turned off (so when the air is not heated by the condenser and not cooled by the evaporator, processes 1-2 and 6-7 of Figure 2 respectively).

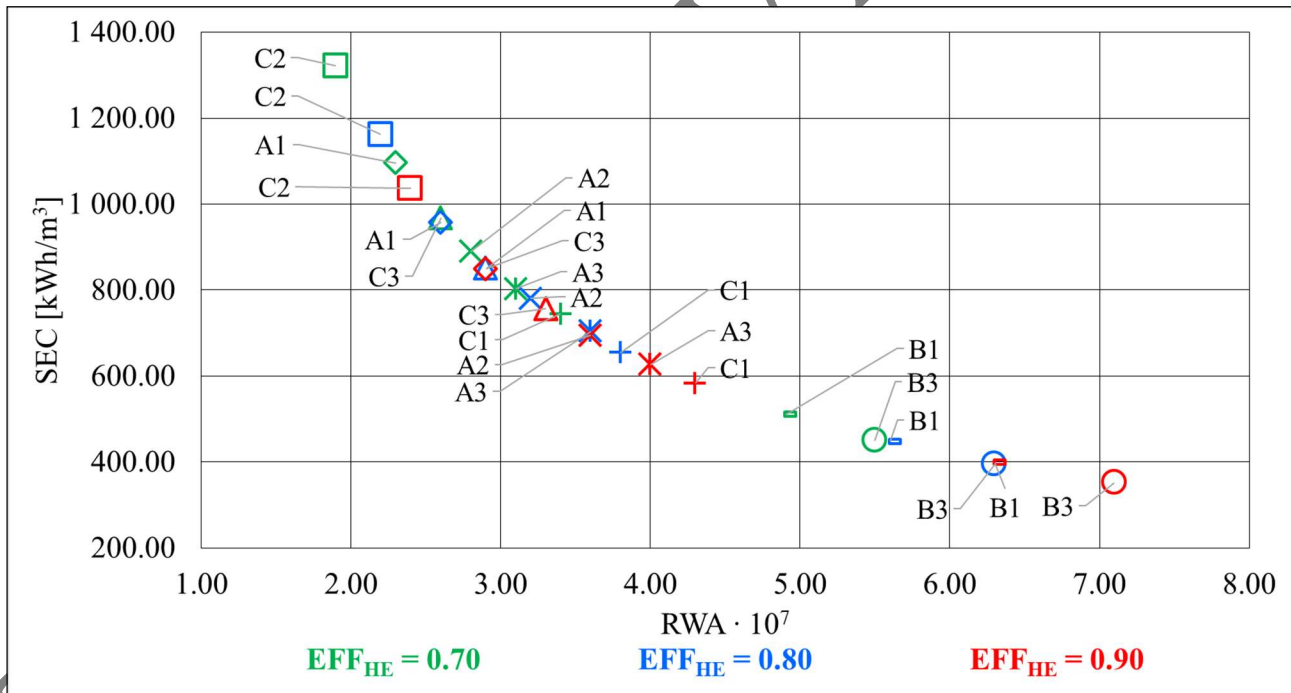


**Figure 12. Performances of the system without VCR cycle in different climate regions of the world.**

Comparing Figures 11 and 12 it is possible to note, for an efficiency of the heat exchanger of 70 %, that:

- In humid climates (as Singapore or Rio de Janeiro) the VCR is fundamental, with an increase of RWA by a factor of 15 and a decrease of SEC of 80 %.
- In dry climates (as Tripoli or Abu Dhabi), the VCR leads to an increase of RWA by a factor of 7 and a decrease of SEC of about 50 %.

## Conclusions

In this paper, a numerical model that simulates the operational performance of a novel HDH desalination system, based on the utilization of Indirect Evaporative Cooling (IEC) and Vapour Compression Refrigeration (VCR) cycle, has been realised. The IEC technology has an unexplored potential for the desalination processes: the secondary air stream can be humidified by seawater evaporation, while the cooled primary stream can be used as source of pre-humidification of the secondary one. A VCR cycle has been introduced in the configuration scheme, to improve the humidification process (pre-heating the air entering the IEC device by the VCR hot coil) and to increase freshwater recovery (cooling and dehumidifying the secondary stream of the IEC device by the VCR cold coil). This novel configuration has been named *Enhanced Indirect Cooling Evaporative Desalination* (EICED) system by the Authors. A simulation code developed in Matlab can solve the equations that rule the functioning of the proposed EICED scheme. The governing equations take into account the different operation modes of the devices, that vary as a function of inlet air conditions. Some significant test points have been considered to investigate and discuss the performance of the systems in real operating conditions. An analysis of the performances in different sites of the world have been conducted. Complying with the admissible operational ranges of the devices, parametric analysis and feasibility analysis in different cities show what follows:

- The highest performance can be reached when inlet air is hot and humid, i.e. for a test inlet point with temperature and humidity ratio equal to 35.0 °C and 0.016 kg/kg, a GOR of 3.4 and an RWA of  $5.0 \cdot 10^6$  has been calculated.
- The VCR cycle greatly improves the desalination performance of the system and quite similar results are obtainable in many climates around the world; comparing an humid climate (i.e. Singapore) with a dry one (i.e. Abu Dhabi) GOR of 3.15 and 2.98, RWA of  $4.10 \cdot 10^6$  and  $4.00 \cdot 10^6$ , are respectively achievable.

It is essential to highlight that, in this work, the efficiency parameters account for the energy consumed for the air movement (equal to the energy needs of the IEC device) that, in general, is neglected in the HDH systems literature works. Despite this, the proposed EICED scheme still shows very promising performance indices among HDH desalination technology, even if they are worse respect to reverse osmosis (SEC of about 4.0 kWh/m<sup>3</sup> [5]), which is the most common desalination technology.

Definitely, taking in account the advantages of HDH technology (no extensive maintenance, no limitation of water salinity, possibility to employ low-grade energy), it is very important to investigate possible novel HDH configurations: in this sense, the results obtained in this paper open up a new perspective towards the widespread use of EICED technology in the desalination sector.

## Acknowledgements

The Authors would like to thank *Seeley International* (<https://www.seeleyinternational.com/eu/corporate/emea/>), for all the precious support in the realisation of this work.

## References

- [1] N. Voutchkov, *Desalination Engineering - Planning and design*, McGraw Hill, 2013.
- [2] M. A. Abdelkareem, M. El Haj Assad, E. T. Sayed, B. Soudan, *Recent progress in the use of renewable energy sources to power water desalination plants*, Desalination, 2018.  
<https://doi.org/10.1016/j.desal.2017.11.018>
- [3] C. Felter, K. Robinson, *Water Stress: A Global Problem That's Getting Worse*, Council on Foreign Relations, 2021. <https://www.cfr.org/backgrounder/water-stress-global-problem-thats-getting-worse>
- [4] N. Voutchkov, *Desalination Engineering - Operation and maintenance*, McGraw Hill, 2014.
- [5] J. Eke, A. Yusuf, A. Giwa, A. Sodi, *The global status of desalination: An assessment of current desalination technologies, plants and capacity*, Desalination, 2020.  
<https://doi.org/10.1016/j.desal.2020.114633>
- [6] FAO United Nations, *FAO's Global Information System on Water and Agriculture*.  
<http://www.fao.org/aquastat/en/overview/methodology/water-use>
- [7] Our world in data, *Water use and stress*. <https://ourworldindata.org/water-use-stress>
- [8] M. N. Soliman, F. Z. Guen, S. A. Ahmed, H. Saleem, M. J. Khalil, S. J. Zaidi, *Energy consumption and environmental impact assessment of desalination plants and brine disposal strategies*, Process Safety and Environmental Protection, 2021.  
<https://doi.org/10.1016/j.psep.2020.12.038>
- [9] M. Faegh, P. Behnam, M. B. Shafii, *A review on recent advances in humidification-dehumidification (HDH) desalination systems integrated with refrigeration, power and desalination technologies*, Energy Conversion and Management, 2019.  
<https://doi.org/10.1016/j.enconman.2019.06.063>
- [10] P. Narayan, J. Lienhard, *Humidification Dehumidification Desalination*, Wiley, 2014.
- [11] S. M. Zubair, M. A. Antar, S. M. Elmutasim, D. U. Lawal, *Performance evaluation of humidification-dehumidification (HDH) desalination systems with and without heat recovery options: An experimental and theoretical investigation*, Desalination, 2018.  
<https://doi.org/10.1016/j.desal.2018.02.018>
- [12] M. Sharqawy, M. Antar, S.M. Zubair, A. Elbashir, *Optimum thermal design of humidification dehumidification desalination systems*, Desalination, 2014.  
<http://dx.doi.org/10.1016/j.desal.2014.06.016>
- [13] P. G. Narayan, M. H. Sharqawy, E.K.Summers, J.Lienhard, S.M.Zubair, M.Antar, *The potential of solar-driven humidification-dehumidification desalination for small-scale decentralized water production*, Renewable and Sustainable Energy Reviews, 2010.  
<https://doi.org/10.1016/j.rser.2009.11.014>
- [14] H. Müller-Holst, M. Engelhardt, M. Herve, W. Scholkopf, *Solar thermal seawater desalination systems for decentralised use*, Renewable Energy, 1998.  
[https://doi.org/10.1016/S0960-1481\(98\)00083-4](https://doi.org/10.1016/S0960-1481(98)00083-4)
- [15] E. Chafik, *A new type of seawater desalination plants using solar energy*, Desalination, 2003.  
[https://www.researchgate.net/publication/228432616\\_A\\_New\\_Seawater\\_Desalination\\_Process\\_Using\\_Solar\\_Energy](https://www.researchgate.net/publication/228432616_A_New_Seawater_Desalination_Process_Using_Solar_Energy)
- [16] M. H. Mahmood, M. Sultan, T. Miyazaki, S. Koyama, V. S. Maisotsenko, *Overview of the Maisotsenko cycle – A way towards dew point evaporative cooling*, Renewable and Sustainable Energy Reviews, 2016. <http://dx.doi.org/10.1016/j.rser.2016.08.022>
- [17] D. Pandelidis, A. Pacak, S. Anisimov, *Energy saving potential by using Maisotsenko-Cycle in different applications*, International Journal of Earth and Environmental Sciences, 2018.  
<https://doi.org/10.15344/2456-351X/2018/159>
- [18] A. Kabeel, M. Abdelgaied, M. Feddaoui, *Hybrid system of an indirect evaporative air cooler and HDH desalination system assisted by solar energy for remote areas*, Desalination, 2018.  
<https://doi.org/10.1016/j.desal.2018.04.013>

- [19] Q. Chen, M. Burhan, M. Shahzad, D. Ybyraiymkul, F. H. Akhtar, K. C. Ng, *Simultaneous production of cooling and freshwater by an integrated indirect evaporative cooling and humidification-dehumidification desalination cycle*, Energy Conversion and Management, 2020. <https://doi.org/10.1016/j.enconman.2020.113169>
- [20] R. Tariq, N. A. Sheikh, J. Xaman, A. Bassam, *An innovative air saturator for humidification-dehumidification desalination application*, Applied Energy, 2018. <https://doi.org/10.1016/j.apenergy.2018.06.135>
- [21] D. Pandelidis, A. Cichon, A. Pacak, P. Drag, M. Drag, W. Worek, S. Cetin, *Water desalination through the dewpoint evaporative system*, Energy Conversion and Management, 2020. <https://doi.org/10.1016/j.enconman.2020.113757>
- [22] S. Nada, H. Elattar, A. Fouda, *Experimental study for hybrid humidification–dehumidification water desalination and air conditioning system*, Desalination, 2015. <http://dx.doi.org/10.1016/j.desal.2015.01.032>
- [23] H. Elattar, A. Fouda, S. Nada, *Performance investigation of a novel solar hybrid air conditioning and humidification-dehumidification water desalination system*, Desalination, 2016. <http://dx.doi.org/10.1016/j.desal.2015.12.023>
- [24] A. Fouda, S. Nada, H. Elattar, *An integrated A/C and HDH water desalination system assisted by solar energy: transient analysis and economical study*, Applied Thermal Engineering, 2016. <http://dx.doi.org/10.1016/j.applthermaleng.2016.08.026>
- [25] S. Nada, H. Elattar, A. Fouda, *Performance analysis of proposed hybrid air conditioning and humidification–dehumidification systems for energy saving and water production in hot and dry climatic regions*, Energy Conversion and Management, 2015. <http://dx.doi.org/10.1016/j.enconman.2015.02.082>
- [26] D. Lawal, M. Antar, A. Khalifa, S. Zubair, F. Al-Sulaiman, *Humidification-dehumidification desalination system operated by a heat pump*, Energy Conversion and Management, 2018. <https://doi.org/10.1016/j.enconman.2018.01.067>
- [27] D. Lawal, M. Antar, S. Zubair, *Exergo-economic analysis of humidification-dehumidification (HDH) desalination systems driven by heat pump (HP)*, Desalination, 2018. <https://doi.org/10.1016/j.desal.2018.05.011>
- [28] Seeley International, *CW H Technical Specifications*. <https://www.seeleyinternational.com/artefact/cwh-technical-specifications-metric/>
- [29] Seeley International, *Climate Wizard Calculator*. <https://www.seeleyinternational.com/commercial/tools/>
- [30] Energy Plus, *Engineering Reference*. <https://energyplus.net/documentation>
- [31] Big Ladder Software, *Output Details and Examples - DXCoolingCoil*, <https://bigladdersoftware.com/epx/docs/9-5/output-details-and-examples/simple-list-data-sets.html#dxcoolingcoil.idf>
- [32] Modelica Buildings Library, *Performance data for SingleSpeed DXCoils - Carrier Centurion 50PG06*. [https://simulationresearch.lbl.gov/modelica/releases/v4.0.0/help/Buildings\\_Fluid\\_HeatExchangers\\_DXCoils\\_AirCooled\\_Data\\_SingleSpeed.html#Buildings.Fluid.HeatExchangers.DXCoils.AirCooled.Data.SingleSpeed.Carrier\\_Weathermaster\\_50HJ006](https://simulationresearch.lbl.gov/modelica/releases/v4.0.0/help/Buildings_Fluid_HeatExchangers_DXCoils_AirCooled_Data_SingleSpeed.html#Buildings.Fluid.HeatExchangers.DXCoils.AirCooled.Data.SingleSpeed.Carrier_Weathermaster_50HJ006)
- [33] Carrier, *Carrier Centurion Product Data 50PG03-28*. <http://www.aireclima.com/carrier/pdf/50PG-5PD.pdf>
- [34] J. A. Arnfield, *Köppen climate classification*, Encyclopedia Britannica, 2020. <https://www.britannica.com/science/Koppen-climate-classification>
- [35] Energy Plus, *Energy Plus Weather Data*. <https://energyplus.net/weather>